Journal of Nuclear Materials 378 (2008) 273–281

Contents lists available at ScienceDirect

Journal of Nuclear Materials

journal homepage: www.elsevier.com/locate/jnucmat

Microstructural stability of modified 9Cr–1Mo steel during long term exposures at elevated temperatures

V. Thomas Paul, S. Saroja *, M. Vijayalakshmi

Physical Metallurgy Division, Metallurgy and Materials Group, Indira Gandhi Centre for Atomic Research, Kalpakkam 603 102, India

ARTICLE INFO

Article history:
Received 13 February 2008
Accepted 4 June 2008

PACS:
81.40.Ef
68.37.Lp
61.05.Jm

ABSTRACT

This paper describes the stability of microstructure in normalized and tempered modified 9Cr–1Mo steel exposed to service temperatures in the range of 773–873 K for different time durations. A detailed microstructural and microchemical analysis of the secondary phases was carried out using optical and electron microscopy techniques. The microstructural observations, supported by hardness measurements showed that the lath morphology of the tempered martensite was retained even after 10000 h of aging. The coarsening of $M_{23}C_6$ carbide was observed until 5000 h, when the Laves phase started appearing. The microstructural features observed are discussed in conjunction with the embrittlement observed in this steel on high temperature aging exceeding 5000 h.

1. Introduction

Ferritic steels especially 9Cr–1Mo steel and its variants are widely used in power industries due to their acceptable high temperature creep strength, good resistance towards oxidation and stress corrosion cracking, adequate fracture toughness and reasonable cost. The present generation of ferritic steels pertains to the 7–12%Cr ferritic/martensitic steels, where the most crucial parameters are the high temperature strength and creep resistance. Interest in tempered ferritic/martensitic steels for nuclear applications especially for high burn up fast breeder reactors, generation IV reactors and fusion reactors has increased considerably in the recent years in view of their excellent resistance to void swelling, thermal and irradiation creep and fatigue, compared to their austenitic counter-parts. [1–3]. Rapid strides have been made the world over in the design and development of advanced ferritic martensitic steels by modification of chemistry and processing methods. The high chromium 9–12% ferritic martensitic steels are being developed with continuous improvements in performance by optimization of carbon content, addition of solid solution strengtheners Mo and W, carbide forming elements Nb and V, partial substitution of Mo by W and controlled addition of elements like N (0.03–0.05 wt%) and B for enhanced creep strength and stability of microstructure.

Modified 9Cr-1Mo steels in which V and Nb contents have been optimized, are being used throughout the world for super heater tubings, and pipings of such plants with steam temperatures up to 866 K [4–6]. However, it is reported that thermal aging at temperatures above 773 K causes gradual but continuous degradation in upper shelf properties in addition to increase in the DBTT [7–9]. It is also well established that the fracture toughness of many power plant steels deteriorate during service at elevated temperatures. These changes are due to two reasons: (i) evolution of carbides and intermetallic phases and (ii) segregation of tramp elements (like P, As, Sn, etc.) to prior austenite grain boundaries. Methods to overcome this problem could be by selection of high purity steel, adoption of double or triple vacuum melting for steel making, strict control of tramp and volatile elements and development of special processing methods, which would improve the nature of grain boundaries. The segregation can be minimized by adopting suitable thermo-mechanical treatments, which can provide a fine and even distribution of these deleterious elements [10,11]. The extent of segregation is found to be low at martensite lath boundaries than at prior austenite grain boundaries. In high chromium martensitic steels, the embrittlement and observed inter-granular failures have been explained by decohesion of grain boundaries enhanced by P segregation, since laves phase is not observed in these steels [12,13]. However, long term aging near the operating temperatures in plain 9Cr–1Mo steel have shown that the formation of laves phase on grain and lath boundaries has a prominent effect than segregation of metalloids [14].

Further, the coarsening of carbides and the precipitation of brittle intermetallic phases along the grain boundaries cause progressive changes in the tempered martensitic microstructure and are prominent factors that deteriorate the fracture properties of the steel. Secondly, martensitic transformation from austenite occurs with the disciplined motion of atoms. Such movements cannot

* Corresponding author. Tel.: +91 44 27480306; fax: +91 44 27480112.
E-mail address: saroja@igcar.gov.in (S. Saroja).

0022-3115/$ - see front matter © 2008 Elsevier B.V. All rights reserved.
doi:10.1016/j.jnucmat.2008.06.033

Table 1
Chemical composition of the steel (in wt%)

Cr	Mo	C	Mn	Si	S	Fe
9.29	0.92	0.097	0.37	0.31	0.0047	Balance
P	Ni	Al	N	V	Nb	
0.018	0.38	0.006	0.057	0.26	0.08	

be sustained across prior austenite boundaries. These prior austenite boundaries become susceptible to impurity segregation and embrittlement. The degree of disorder at the prior austenite grain boundaries is higher than that associated with martensite-martensite boundaries. This is because adjacent martensite laths have coherence with the parent austenite grain and hence a good fit

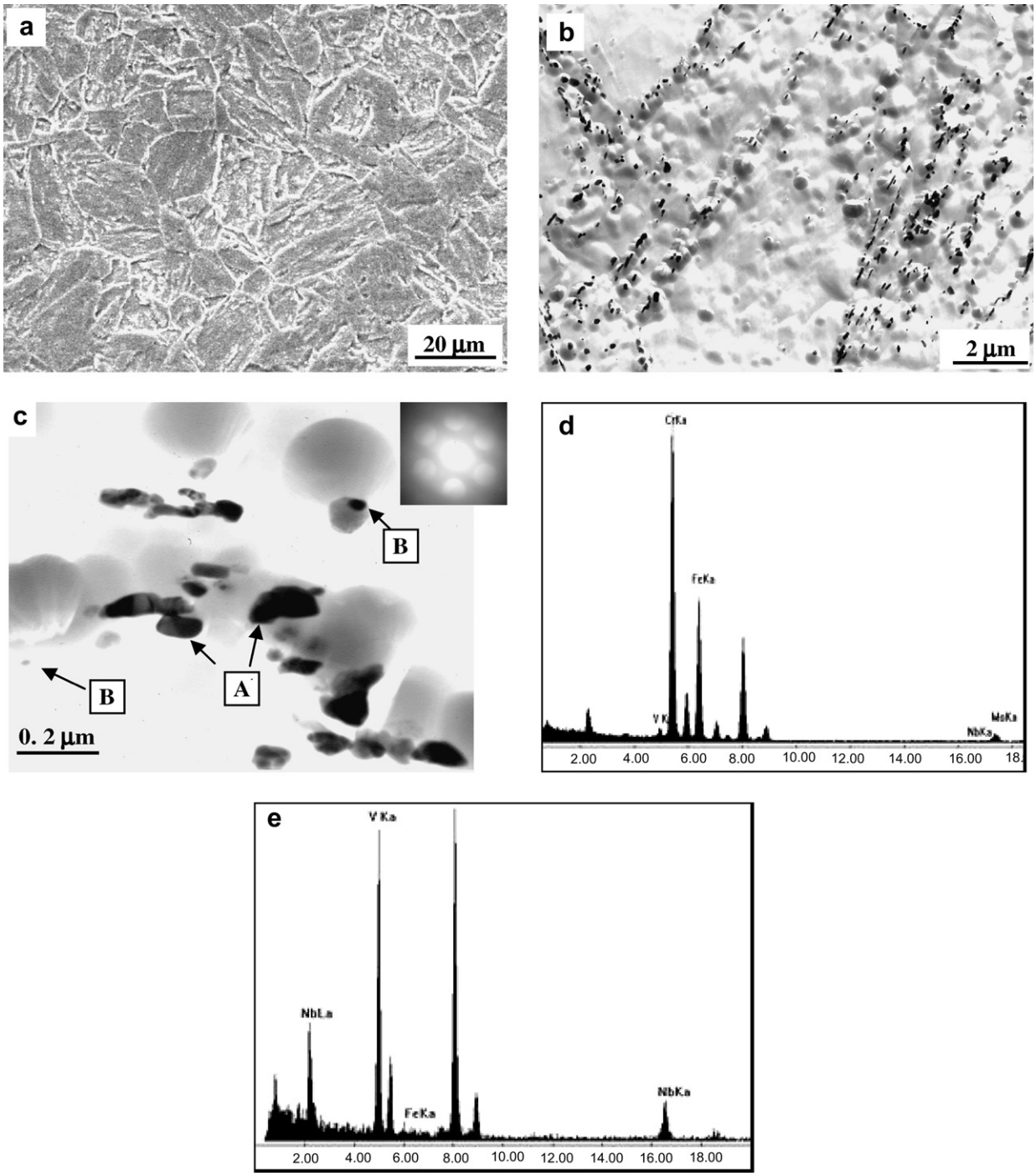

Fig. 1. Microstructure and microchemistry of secondary phases and its locations of normalized and tempered modified 9Cr–1Mo steel: (a) prior austenite grain boundaries and tempered martensitic matrix, (b) carbides on prior austenite and lath boundaries, (c) Coarse $M_{23}C_6$ (diffraction pattern along $\langle \bar{1}\,1\,1 \rangle$ zone axis is given as inset) marked A and fine MX, marked B (d) EDS spectra from Cr rich $M_{23}C_6$ carbide and (e) EDS spectra from V (Nb) rich MX.

with each other, whereas the orientation relationships between austenite grains can be random.

An understanding of the microstructural and microchemical changes during thermal exposure is necessary to assess the stability and performance of the steel for an industrial application. A detailed study on microstructural evolution in modified 9Cr–1Mo steel at different temperatures and time durations has been carried out. The nature, amount and microchemistry of secondary phases were determined. Based on these studies, an attempt is being made to obtain a correlation between the microstructural parameters and possible embrittlement mechanisms in modified 9Cr–1Mo steel are discussed.

2. Experimental

The modified 9Cr–1Mo steel (P91) used in the present study was supplied in the normalized and tempered condition by M/s Rourkela Steel Plant, India in the form of 12 mm thick plates. The chemical composition of the steel is given in Table 1.

Specimen of dimensions 100 mm × 50 mm × 12 mm were fabricated from the plate. The specimens were subjected to a normalization treatment for 1 h at 1333 K followed by a tempering treatment for 1 h at 1023 K to obtain a uniform initial microstructure. Further, the normalized and tempered steel was aged at 773, 823 and 873 K for durations ranging from 500 to 10 000 h in a muffle furnace with a temperature tolerance of ±5 °C.

The heat treated specimens were prepared metallographically by standard preparation procedures. Optical microscopy and hardness measurements were carried out using a Leica MeF4A microscope and Vickers Hardness Testing machine under an applied load of 10 kg. The Prior Austenite Grain Size (PAGS) were measured by the standard linear intercept method. Surface morphology was studied by Scanning Electron Microscopy in a FEI XL 30 ESEM with Energy Dispersive Spectroscopy. Analytical Transmission Electron Microscopy (ATEM) was carried out on thin foils to study the structure and on extraction replicas to identify the type and chemistry of secondary phases. Thin foil for transmission microscopy was prepared by window thinning method using 10% perchloric acid in methanol as electrolyte. Extraction replicas were prepared from well polished and carbon coated specimens using Vilella's reagent. ATEM was carried out using a Philips CM 200 microscope with a SUTW EDS under an operating voltage of 120–160 kV. Precipitates were identified by a combination of electron diffraction and EDS analysis. Quantification of the EDS spectra was done by the Cliff Lorimer method using K_{AB} values generated from standard samples of known chemical composition [15].

3. Results and discussion

The results are presented in the following sequence: (i) characterization of the normalized and tempered modified 9Cr–1Mo steel (ii) microstructural evolution during thermal aging and (iii) variation in microstructural and microchemical parameters.

3.1. Characterization of the normalized and tempered steel

The SEM micrograph of the normalized and tempered modified 9Cr–1Mo steel is shown in Fig. 1(a). The micrograph reveals prior austenite grain boundaries and a tempered martensitic microstructure. Measurement of PAGS showed an average value of about 20 μm. The lower PAGS as compared to plain 9Cr–1Mo steel

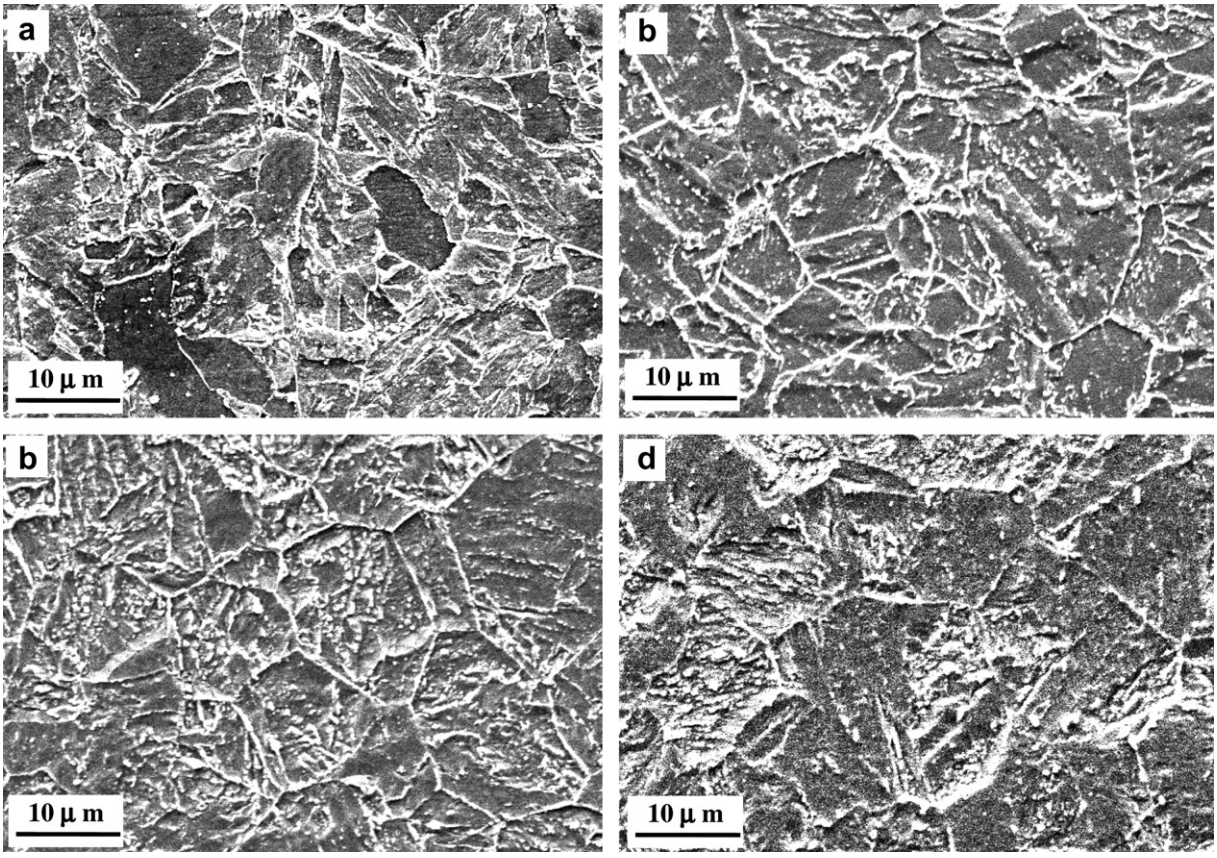

Fig. 2. SEM micrographs of modified 9Cr–1Mo steel aged at different temperatures for short and long durations: (a) 773 K for 500 h, (b) 873 for 500 h, (c) 773 for 10 000 h and (d) 873 for 10 000 h.

(~40 μm) [16] is attributed to the presence of un-dissolved carbides along the austenite grain boundaries during normalization treatment, which inhibit the growth of austenite grains. As per THERMOCALC prediction of equilibrium phases in modified 9Cr–1Mo steel, MX precipitates may be stable even at the austenitizing temperature of 1333 K [17]. Carbide agglomerates were seen along the prior austenite boundaries. The average hardness of the steel was found to be 240 ± 5VHN. The relatively higher hardness value of tempered martensite as compared to plain 9Cr–1Mo steel [18] may be due to fine grain size and abundance of precipitates. In order to understand the type and chemistry of the carbide, detailed analytical transmission electron microscopy (ATEM) was carried out on extracted carbon replicas.

Fig. 1(b) shows the distribution of carbides in the tempered steel. Both inter and intra granular precipitates of different morphologies like globular, cylindrical to lenticular are observed in the figure. Most of the intra granular precipitates were aligned along the lath boundaries. But very fine intra lath precipitates were also observed at higher magnifications (Fig. 1(c)).

The crystal structure/type of various carbides was identified using micro-diffraction due to their fine size. The diffraction pattern taken along $\langle \bar{1}\,1\,1 \rangle$ from a coarse globular carbide (Fig. 1(c)) is shown as an inset. Analysis of the pattern showed that it belonged to the fcc carbide $M_{23}C_6$, the most common carbide observed in this steel. Analysis of diffraction patterns from a number of carbides on grain/lath boundaries with cylindrical or lenticular shape showed that they belonged to the same $M_{23}C_6$ type. The sizes of the carbides varied from 25 to 150 nm diameter in the case of globular carbides and 200–250 nm width in the case of lenticular carbides.

Diffraction analysis on few carbides, that formed at the martensitic lath interfaces and within the laths showed that they are of MX type. These carbides were found to be very fine (20–30 nm) as compared to $M_{23}C_6$. The presence of very fine precipitate along the lath interface would prevent the migration of interface during long term exposures and thereby impart good high temperature properties. The MX carbides precipitate within sub grains during tempering and increase the creep strength by pinning down the moving dislocations, due to their fine size. The higher thermal stability of MX favors the use of this steel for high temperature applications.

The EDS spectrum from the carbide, marked 'A' in Fig. 1(c) is shown in Fig. 1(d). The $M_{23}C_6$ carbides were found to be rich in Cr, with small amounts of Mo and Fe in solution. The average Cr/Fe ratio in these carbides was found to be 1.937. This is in agreement with earlier studies carried out on plain 9Cr–1Mo steels in our laboratory and on P91 by others groups [18–20].

The EDS spectrum from a fine intra lath precipitate is shown in Fig. 1(e). It is observed to be Vanadium rich, although the presence of Niobium is also observed. This suggests that these fine carbides are of MX type. Although most of the MX type of carbides was V rich, a few Nb rich precipitates were also observed. Interestingly, equilibrium calculations indicated that the strengthening effect of V in similar steels is derived from VN [17]. Since the identity of X could not be obtained in the present study it is generally designated as carbo-nitrides. The ratio of concentration of niobium to vanadium in MX was found to vary from 0 to 1. Based on the above results, the microstructure of normalized and tempered modified 9Cr–1Mo can be summarized as tempered martensite, $M_{23}C_6$ and MX. The stability of this microstructure during thermal exposure is discussed in the next section.

3.2. Microstructural evolution during thermal aging

Study of microstructural changes in P91 during long term aging are of importance since it has been reported [14] that plain 9Cr–1Mo steel is susceptible to embrittlement. The tendency for embrittlement in plain 9Cr–1Mo steel is reported to be highest around 823 K. Hence, the present steel has been subjected to aging in the temperature range of 773–873 K. Thermal exposure in this temperature range is expected to cause softening of the steel and variations in the size, number density of carbides and their microchemistry. This section deals with the microstructural evolution, while resultant changes in the microstructural and microchemical parameters are discussed in the subsequent section.

Typical SEM micrographs of the steel aged at 773 and 873 K for different durations (500 and 10 000 h) are shown in Fig. 2. Though a tempered martensitic structure with retention of lath morphology is observed in all cases, signatures of a gradual and steady recovery is clear from the micrographs. Relatively coarser grains with precipitation of coarse carbides along the prior lath boundaries are clearly seen after aging for 10000 h. The hardness of the steel aged at 773 K was 249 and 247VHN for 500 h and 1000 h, respectively, while at 873 K it was 249 and 253VHN for the two durations. The hardness values indicate saturation. This suggests that the softening effect due to recovery has been offset by other changes that increase the hardness, which could be due to formation of secondary phases.

Fig. 3 shows the thin foil TEM micrograph of the steel aged at 773 K for 10 000 h. Several regions of the steel are showed equiaxed ferrite grains with a preponderance of secondary phases. Although considerable re-crystallization had taken place the

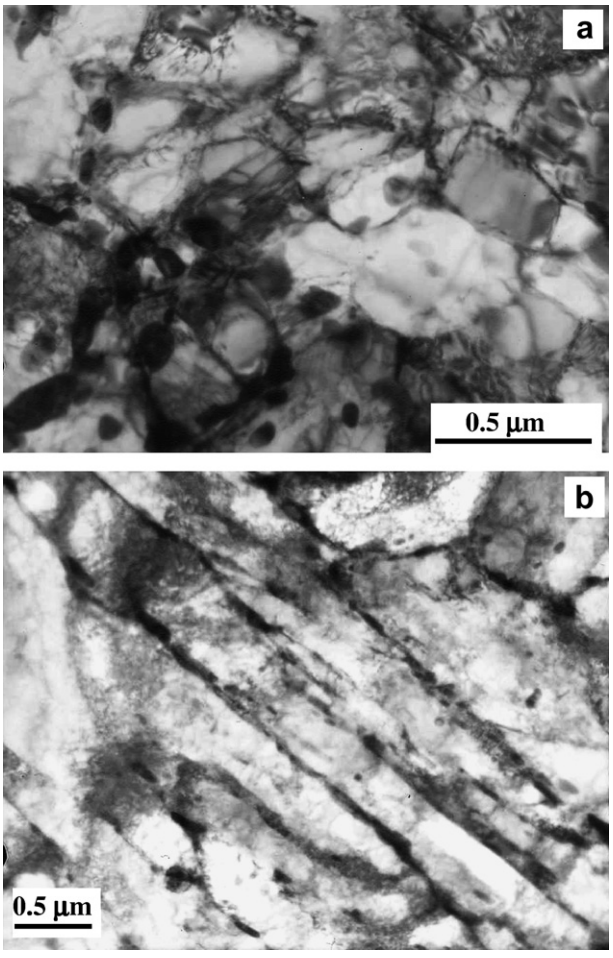

Fig. 3. TEM micrographs from 773 K/10 000 h aged steel showing: (a) polygonised ferrite grains and carbides and (b) evidence for lath structure at adjacent to ferrite grains.

initial lath structure was not completely erased from the steel even after 10 000 h of aging, which together with the presence of fine carbides could be a reason for the observed value of hardness. The micrographs from carbon extraction replica in Fig. 4 show the size and distribution of carbides in the steel aged at 773 K for 500 h, 5000 h and 10 000 h. Though the number density of carbides did not change appreciably up to 5000 h at 773 K (Fig. 4(b)) it was found to be high at 10 000 h (Fig. 4(c)). The predominant secondary phase was identified as Cr rich $M_{23}C_6$ from EDS (not shown) and diffraction (left inset of Fig. 4(a)) analysis. In addition, very fine precipitates were present mainly within the laths and lath boundaries at all temperatures. Inset (right) of Fig. 4(a) shows a typical diffraction pattern from such a carbide taken along $\langle \bar{1}\,1\,2 \rangle$ zone axis. These were analyzed as MX type of carbides. These mono carbides were found to be rich in either Nb/V rich or both.

In addition to the MX and $M_{23}C_6$ carbides the presence of fine precipitates especially along the grain boundaries (inset of Fig. 4(b)) was observed after aging for 5000 h at 773 K. By diffraction (inset of Fig. 4(b)) analysis they were identified as Laves phase of A_2B type having a c.p.h structure. EDS analysis (Fig. 4(d)) shows that they are rich in Fe and Mo with small amount of Si. Based on the analysis of a large number of such precipitates, $(Fe,Si)_2$ Mo type of spectra is found to be characteristic of the Laves phase, which can be used as a 'finger print' for identification of Laves phase. It is also reported that Si promotes the formation of Laves phase in similar steel during aging [14,23]. Further, aging up to 10 000 h at 773 K revealed the presence of a thin sheet network of Laves phase (inset of Fig. 4(c)) along the prior austenite grain boundaries. It can be understood that the presence of fine precipitates or layers of Laves phase could also have offset the softening effect due to aging and could be responsible for the reported loss of toughness [21–25] or reduction in Upper Shelf Energy in the impact tested modified 9Cr–1Mo steel [26].

Aging at 823 K resulted in a similar microstructure, consisting of tempered martensite, $M_{23}C_6$ and MX carbides in specimen aged up to 1000 h. The number density of carbides was comparable to that at 773 K. The Laves phase, which was observed after 5000 h was however more widespread as compared to 773 K. Careful TEM examinations revealed that Laves phase formed as bridges between the existing grain boundary carbides (Fig. 5(b)). Additionally, Laves phase also formed along the lath boundaries in addition to prior austenite grain boundaries at 10 000 h. The EDS spectra from various regions of coarse carbides showed that some of them are encapsulated within a thin layer of Laves phase. This has been confirmed by X-ray maps of the precipitates in a carbon extraction replica, which is described in the next section.

Increase in aging temperature to 873 K did not show any considerable effect for short durations. Fig. 5(a) shows the TEM micrograph from a carbon extraction replica of the steel aged for 1000 h at 873 K. The carbides (especially lath boundary globular carbides) are found to be coarse as compared to that

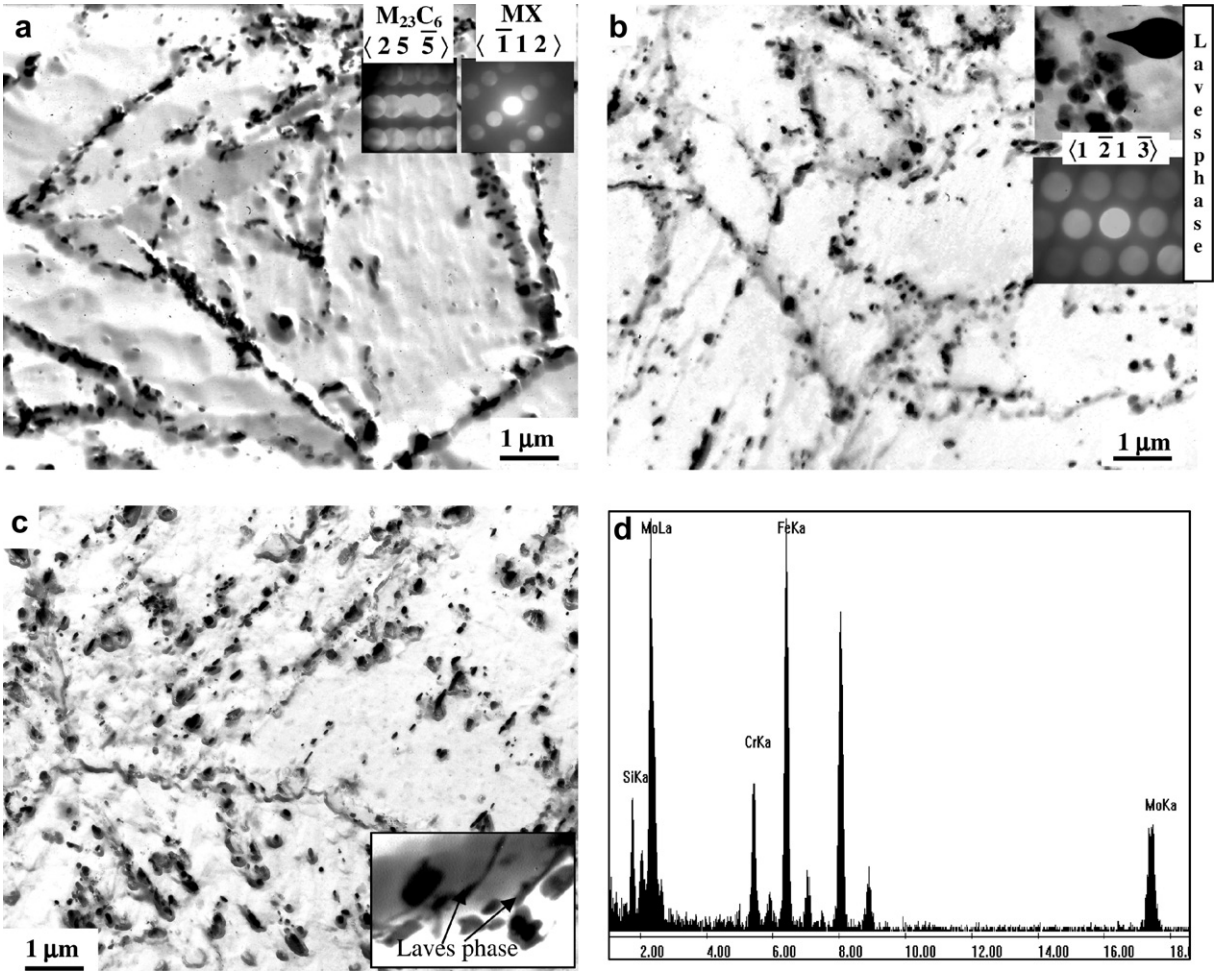

Fig. 4. Distribution of carbides after aging at 773 K for durations: (a) 1000 h (insets – diffraction patterns from $M_{23}C_6$ and MX type carbides taken along $\langle 2\,5\,\bar{5} \rangle$ and $\langle \bar{1}\,1\,2 \rangle$ zones axis, respectively), (b) 5000 h (inset – showing Laves phase, pattern from Laves phase along $\langle 1\,\bar{2}\,1\,\bar{3} \rangle$ zone axis)), (c) 10 000 h, showing higher number density of carbides (inset- showing thin sheets of Laves phase network along grain boundaries) and (d) EDS spectrum taken from laves phase particle shown in the inset of (b).

at 773 K. Additionally, fine lenticular carbides were also found to have freshly precipitated along the lath boundaries as seen in Fig. 5(a). Although coarsening was observed at 873 K/1000 h, decrease in the number density of carbide was not apparent, which could be due to the fresh precipitation of carbides along the lath boundaries. Spheroidisation of carbides (Fig. 5(b)) was evident at 5000 h and beyond. Laves phase was also observed along the boundaries after 5000 h of aging. Fig. 5(c) shows the micrograph after 10000 h aging at 873 K. A continuous network of carbides and Laves phase along the prior austenite grain boundaries is seen. Hardness of the steel aged for 5000 and 10000 h at 873 K was found to be 238 and 243VHN, respectively. This is in agreement with the expected hardness trend wherein softening due to coarsening of $M_{23}C_6$ carbides is compensated by the precipitation of fresh carbides/Laves phases, resulting in a near constancy in hardness levels.

3.2.1. Identification of Laves phase by X-ray mapping

As stated earlier the Laves phase was found to be rich in both Fe and Mo, while $M_{23}C_6$ was rich in Cr and lean in Fe. Using microchemistry as a guideline, X-ray maps were generated to determine the mechanism and preferential nucleation sites for the Laves phase. Fig. 6 shows the Fe, Cr and Mo X-ray images and the electron image from a specimen aged for 5000 h at 873 K.

The enrichment of Cr in Fig. 6(a) in the core of the precipitate is typical of that of $M_{23}C_6$ carbide. The enrichment of Fe (Fig. 6(b)) and Mo (Fig. 6(c)) at the periphery of the grain boundary carbide suggests that a different phase is surrounding the $M_{23}C_6$. This observation together with diffraction (Fig. 5(b)) results suggests that Fe-Mo rich Laves phase forms like a shell encapsulating an $M_{23}C_6$ particle. The formation of Laves phase after 5000 h of aging could also be responsible for the sluggish growth of $M_{23}C_6$ after 5000 h [27]. Fig. 7 shows a comparison of grain sizes for different aging temperatures and time. A decrease in the rate of coarsening of $M_{23}C_6$ carbide after 5000 h is observed from Fig. 7. In other words, the localized decrease in supersaturated carbon available for precipitation or growth of $M_{23}C_6$ in the matrix initiates the precipitation of carbon free Laves phase.

The observed abundance of Laves phase in the present steel can be explained by the relative higher silicon (0.31%) content, as silicon promotes the formation of this phase. Extensive precipitation of Laves phase deprives the matrix of its Mo content, which is detrimental to the strength of the steel. Laves phase is considered as a potential site for crack initiation and its presence on grain boundaries makes the steel susceptible to intergranular cracking. Precipitation of intermetallic Laves phase and segregation of metalloids on interface boundaries on prolonged aging are possible causes for thermal embrittlement, which manifest either as decrease in USE or increase in DBTT. Further alloying to stabilize the carbides (MC) along with a slight modification in the C (or B) content or a change in the tempering conditions (higher tempering temperature for shorter time leaving more residual carbon in the matrix) are possible methods to reduce Laves phase precipitation.

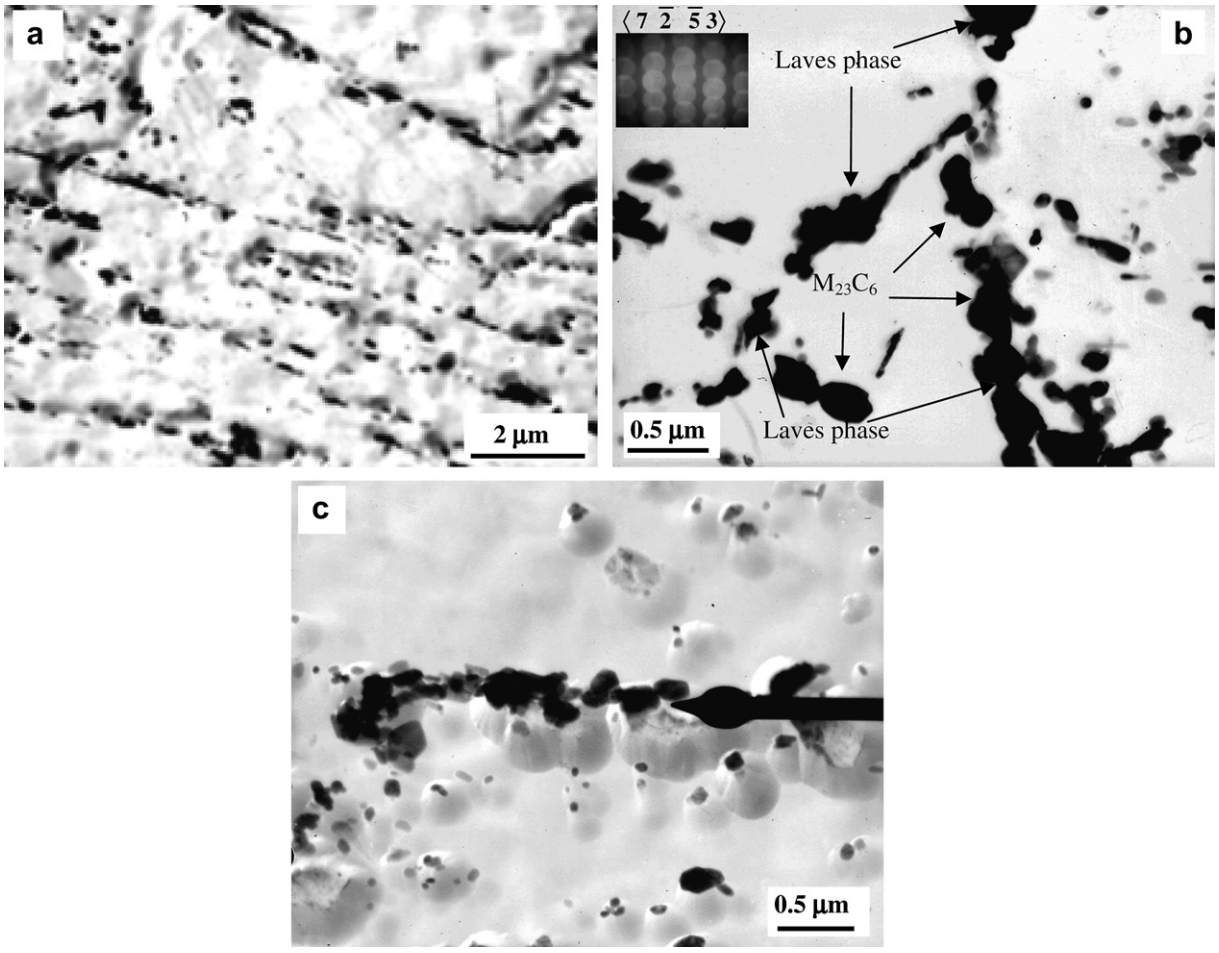

Fig. 5. Distribution of secondary phases after aging at 873 K for: (a) 1000 h of aging, (b) 5000 h of aging (inset shows diffraction pattern along from Laves phase ⟨7 2̄ 5̄ 3⟩ zone axis and (c) 10000 h of aging, showing a continuous network of carbides and Laves phase.

3.3. Evaluation of microstructural and microchemical parameters of secondary phases

The stability of the steel at high temperatures depends upon the integrity of the secondary carbides present. Therefore, a thorough understanding of the changes in microstructural and microchemical parameters at different temperatures and time is necessary. Identification, evaluation of size and chemistry was carried out by analytical transmission electron microscopy. As shown in Fig. 3(a) and Fig. 4(a) most of the carbides were found to be along prior austenite boundaries, although their presence on lath boundaries and intra lath was also observed. Majority of the grain and lath boundary carbides were identified as $M_{23}C_6$. The size of $M_{23}C_6$ on prior austenite boundaries in the normalized and tempered steel was ~150 nm (globular or near globular). The lath boundary carbides were either globular or lenticular, with an average diameter (or width) of ~100 nm. The mono carbides of MX type had typical sizes of ~30 nm and were mostly confined intra lath regions.

The growth profile of the carbides as a function of temperature and time is shown in Fig. 7. It is seen that the growth of $M_{23}C_6$ at grain and lath boundaries is very slow at lower temperature, but grows to a size of 350 nm after 10000 h at 773 K, although the dimensions of mono carbides (MX) remained almost constant even after aging for 10000 h at 873 K. After aging at 873 K for 10000 h most of the grain boundary carbides had grown to a size of about 600 nm, which was almost close to saturation size.

The relative changes in the composition of the carbide with aging time and temperature has been evaluated. The ratio of different elements present in the $M_{23}C_6$ carbide was quantified from EDS spectra and is plotted in Fig. 8. The presence of small amount of V was observed in the $M_{23}C_6$ carbides present in the aged steel. A continuous increase in the Cr/Fe ratio with aging time, with a higher rate of increase at 873 K is clearly seen. This is attributed to the continuous evolution of the metastable $M_{23}C_6$ phase due to thermal activation driven diffusion of chromium into the carbide as it progresses towards attaining the stable configuration of $Cr_{23}C_6$. The continuous increase in Cr/Fe ratio during aging with respect to temperature and time has also been observed in our earlier work on plain 9Cr–1Mo steel [18]. MX carbides were either rich in V or Nb or both at lower temperature and short durations. Interestingly, most of the mono carbides in the 873 K/10000 h aged steel were rich in Nb. This could be due to higher stability of NbC as compared

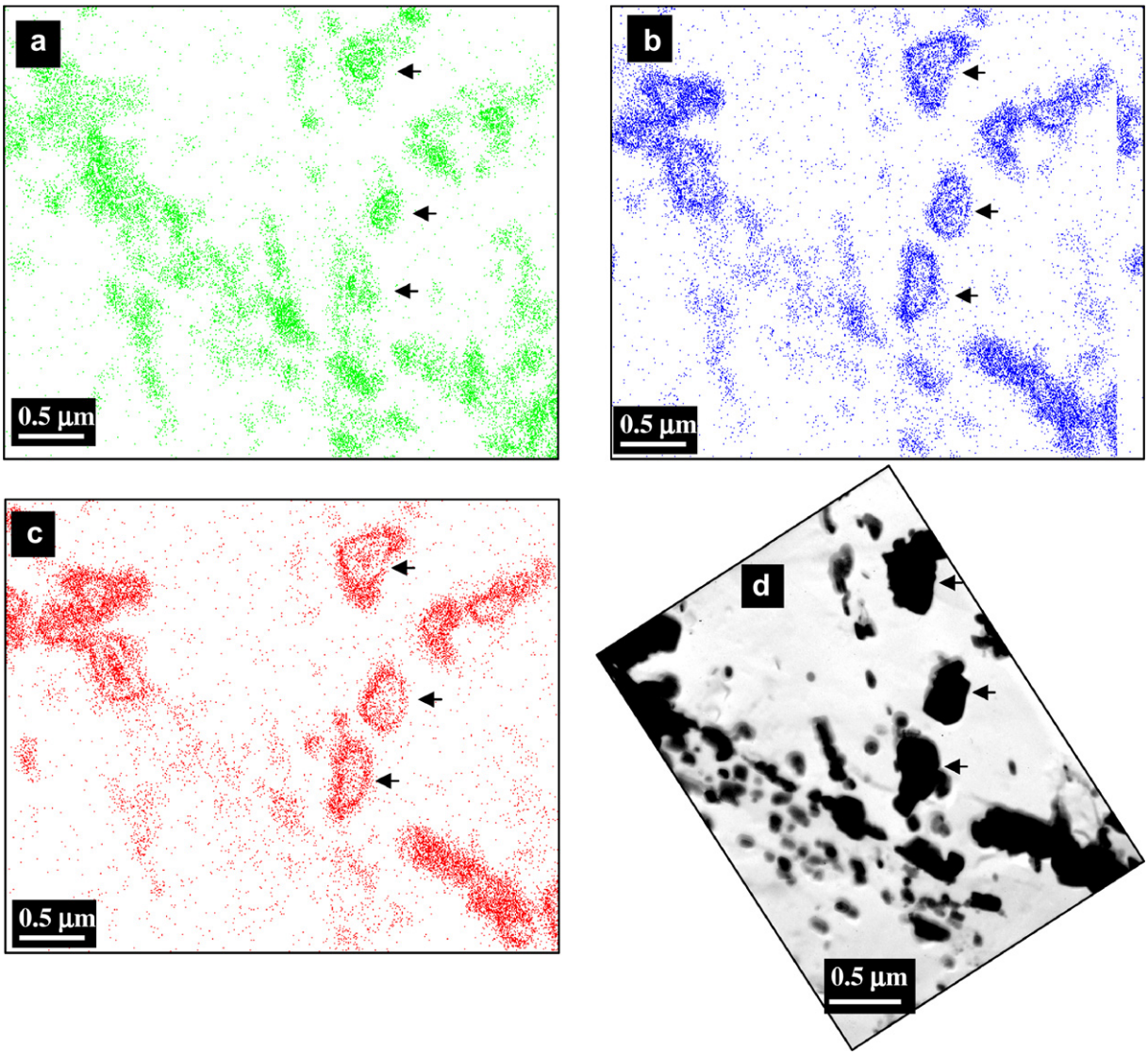

Fig. 6. EDS X-ray maps from secondary phases on a carbon extraction replica of modified 9Cr–1Mo steel aged for of sample aged for 5000 h at 873 K: (a) Cr Lα, (b) Fe Lα, (c) Mo Lα and (d) corresponding TEM bright field image.

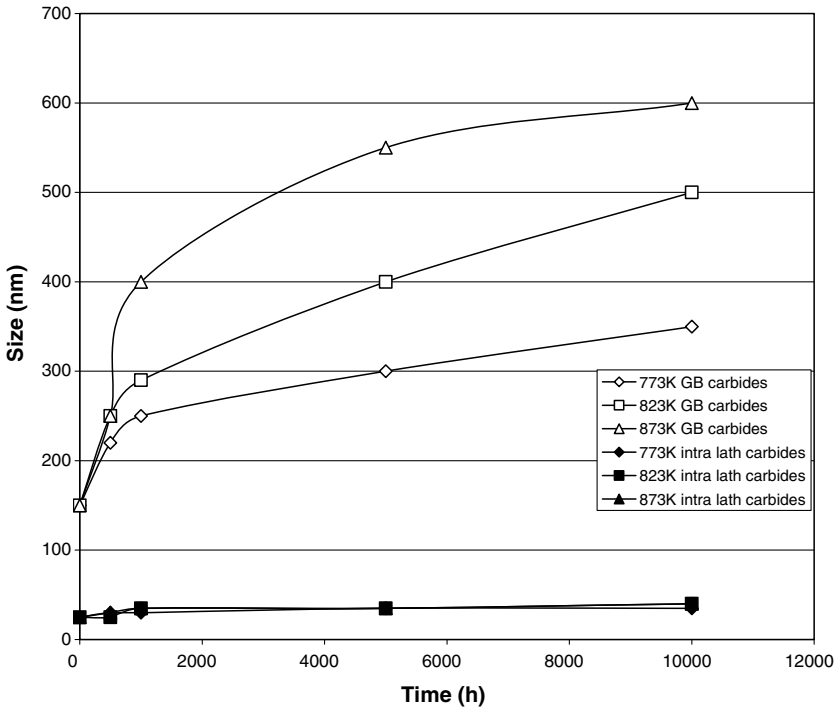

Fig. 7. Growth of carbides as a function of aging temperature and time in modified 9Cr–1Mo steel.

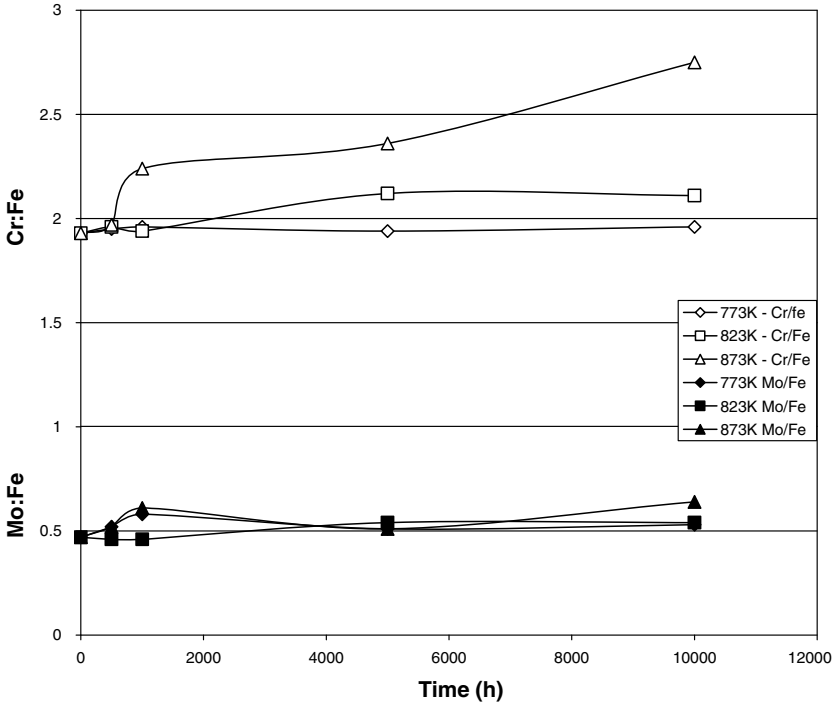

Fig. 8. Compositional variations of $M_{23}C_6$ carbide as a function of aging temperature and time.

to VC carbides. The existence of very stable mono carbides, especially NbC accounts for the resistance of the steel to softening on aging as seen by consistent hardness values. A method to reduce precipitation (either carbides or Laves phase) or an even distribution could be attained by reducing the energy of prior austenite grain boundaries. This could be realized by making the boundaries strongly crystallographically textured or employing grain boundary engineering [4]. Based on the above studies the nature and microchemistry of various secondary phases evolving with time at three different temperatures has been evaluated.

4. Conclusions

The stability of modified 9Cr–1Mo steel on prolonged aging at near service temperatures has been studied in detail. The important conclusions of the study are listed below:

- The lath structure is retained at least certain regions even after 10 000 h of aging at high temperatures.
- Carbides in modified 9Cr–1Mo steel grow with aging time and temperature. The coarsening of V(Nb) carbides was negligible compared to $M_{23}C_6$ carbides.
- Cr/Fe ratio in $M_{23}C_6$ carbides was found to be progressively increasing with time of aging.
- Laves phase appeared after aging for 5000 h and formed a continuous network encompassing the grain boundary carbides with increase in aging time.
- The presence of Laves phase after prolonged aging is a possible reason for the reported decrease in USE and increase in DBTT.

Acknowledgements

The authors would like to express their thanks to Dr Baldev Raj, Director, Indira Gandhi Centre for Atomic Centre, Dr P.R. Vasudeva Rao, Director, Metallurgy and Materials Group and Dr K.B.S. Rao, Associate Director, Materials Development and Characterization Group for their keen interest and constant support.

References

[1] D.R. Harries, in: J.W. Davis, Michel (Eds.), Topical Conference on Ferritic Alloys for Use in Nuclear Energy Techniques, Met. Soc. AIME, Warrendale, 1984, p. 141.
[2] R.L. Klue, K. Ehlich, F. Abe, J. Nucl. Mater. 191–194 (1992) 116.
[3] Baldev Raj, M. Vijayalakshmi, P.R. Vasudeva Rao, K.B.S. Rao, MRS Bull. 33 (4) (2008) 327.
[4] H.K.D.H. Bhadeshia, ISIJ Int. 41 (6) (2001) 626.
[5] R.L. Klueh, D.R. Harries, High-chromium Ferritic and Martensitic Steels for Nuclear applications, ASTM, Monograph 3, 2001.
[6] H. Haneda, F. Masuyama, S. Kaneko, T. Toyoda, in: R. Viswanathan, R.I. Jafffee (Eds.), Advances in Materials Technology for Fossil Power Plants, ASM International, Metals Park, OH, 1997, p. 231.
[7] V.K. Sikka, in: Pressure Vessels and Piping: Materials for Nuclear Steam Generators, ASME, New York, 1985.
[8] D.J. Alexander, P.J. Maziasz, C.R. Brinkman, in: P.K. Liaw et al. (Eds.), Microstructures and Mechanical Properties of Aging Material, TMS, Warrendale, PA, 1993, p. 343.
[9] Hiroyuki Okamura, Ryuiichi Ohtani, Kiyoshi Saito, Kazushige Kimura, Ryuichi Ishii, Kazunari Fujiyama, Shigetada Hongo, Takashi Iseki, Hiroshi Uchida, Nucl. Eng. Des. 193 (1999) 24.
[10] M. Wall, A Review of Thermal Aging Effects in High Chromium Ferritic Steels, UKAEA Report AERE-R 12812, Jan 1987.
[11] Y. Li, Q. Huang, Y. Wu, T. Nagasaka, T. Muroga, J. Nucl. Mater. 367–370 (2007) 117.
[12] V. Foldyna, Z. Kubon, A. Jakovovaand, V. Vodarek, in: A. Strang, D.J. Gooch (Eds.), Microstructural Development and Stability in High Chromium Ferritic Power Plant Steels, The Institute of Materials, London, 1997, p. 73. (Book 667).
[13] T.M. Williams, A.M. Stoneham, D.R. Harries, Met. Sci. 10 (1976) 14.
[14] C.A. Hippsley, N.P. Haworth, Mater. Sci. Technol. 4 (1988) p. 79.
[15] G. Cliff, G.W. Lorimer, Quantitative Microanalysis with High Spatial Resolution, The Metal Society, London, 1981.
[16] S. Saroja, M. Vijayalakshmi, V.S. Raghunathan, Mater. Sci. Eng. A 154 (1992) p. 5.
[17] J. Hald, Steel Res. 67 (9) (1996) 36.
[18] S. Saroja, M. Vijayalakshmi, V.S. Raghunathan, Mater. Trans. JIM 34 (1993) 90.
[19] W.B. Jones, C.R. Hills, D.H. Polonis, Metall. Trans. 22A (1991) 104.
[20] J.M. Vitek, R.L. Klueh, Metall. Trans. 14A (1983) 104.
[21] V. Homolova, J. Janovec, P. Zahumensky, A. Vyrostkova, Mater. Sci. Eng. A 349 (2003) 30.
[22] J.A. Hudson, S.G. Druce, G. Gage, M. Wall, Theor. Appl. Fract. Mech. 10 (1988) 12.
[23] P.J. Maziasz, R.L. Klueh, in: R.E. Stoller et.al. (Ed.), 16th International Symposium, ASTM STP 1125, ASTM, Philadelphia, 1992, p. 1135.
[24] Y. Hosoi, N. Wade, S. Kunimitsu, T. Urita, J. Nucl. Mater. 141–143 (1986) 46.
[25] B.A. Senior, F.W. Noble, B.L. Eyre, Acta Metall. 36 (1988) 185.
[26] M. Wall, C.E. Lane, C.A. Hippsley, Acta Metall. 42 (1994) 129.
[27] P.J. Maziasz, JOM 41 (7) (1989) 1.